micellar solutions: one may be controlled by a chemorheological process involving actual breakdown and reformation of the entanglement network, presumably by scission and re-formation of the threadlike micelles themselves, and the other by disentanglement due to diffusion of the network chains but without accompanying their breakdown.

An important feature of the type III behavior is that the mechanism is a single relaxation time process. This result suggests that the relaxation of the entanglement network of the micellar solutions in the type III region is due to a chemorheological process independent of the length of the threads rather than to a diffusional process highly dependent on the thread length. The peculiar dependence of τ_m on $C_S C_D^{-1}$ of this chemorheological process of entanglement relaxation should reflect the stability of the threadlike micelles under the given environment. In the micellar solutions with $C_S C_D^{-1}$ above 1, the micelles are coexisting with excess NaSal. Therefore, scission and reformation of the micelles may happen rather easily by exchange of the CTAB units of the CTAB/NaSal complexes between the threadlike micelles at the sites of entanglement, where the threadlike micelles can pass through each other with a certain characteristic time (τ_m) reflecting the rate of this process. Scission of the threadlike micelles may also take place, especially in the highly strained portions between entanglement points by the similar mechanism of exchange of the CTAB units with free NaSal molecules in the medium. Since the solubility of CTAB is rather low in the aqueous medium, the exchange rate must be higher; hence the relaxation time is shorter in solutions with a larger excess of NaSal.

Although the detailed features of the dependence of τ_m on $C_S C_D^{-1/2}$ such as seen in Figure 6 cannot be adequately explained at the moment, the general tendency of the C_S and C_D dependences of τ_m and J_e^0 may be interpreted as discussed above.

The type I and type II behavior are the results of the onset of entanglement and the fully developed entanglement network as the threadlike micelles are formed with increasing $C_S C_D^{-1}$ up to the critical value of approximately 1. On the other hand, the type III (Maxwell model) behavior is the result of actual breakdown and re-formation of the entanglement network with the rate dependent on $C_S C_D^{-1/2}$ but with the entanglement density being practically constant after $C_S C_D^{-1}$ exceeds the critical value.

Registry No. CTAB, 57-09-0; NaSal, 54-21-7.

Effects of the Molecular Structure of the Interface and Continuous Phase on Solubilization of Water in Water/Oil Microemulsions

Mean-Jeng Hou and D. O. Shah*

Center for Surface Science and Engineering and Departments of Chemical Engineering and Anesthesiology, University of Florida, Gainesville, Florida 32611

Received February 4, 1987. In Final Form: June 8, 1987

The effects of the molecular structure of the interface and continuous phase on the solubilization capacity of water in water/oil microemulsions have been studied from both theoretical considerations and experimental observations. From the consideration of the thermodynamic stability of microemulsion systems, we have shown that the growth of droplets during the solubilization process is limited at least either by the *spontaneous curvature* of the interface or by the *attractive interaction* among the microemulsion droplets. The influence of the chemical structure of the components on the solubilization capacity was therefore analyzed on the basis of consideration of their effects on the curvature and attraction just mentioned. Experimentally, the solubilization of water in water/oil microemulsions was studied by changing the following variables: molecular volume of oil, chain length, polar head and concentrations of cosurfactants, and salinity. For the systems where the solubilization capacity is limited by the radius of the spontaneous curvature of interface, it was found that the solubilization can be improved by any change in the above variables leading to the decrease of the curvature. For the system where the solubilization capacity is limited by the attractive interaction between microemulsion droplets, any change resulting in the decrease of attractive interaction increases the solubilization capacity. We have further shown that any change in the above-mentioned variables can have opposite effects on the curvature and attraction. Therefore, maximum solubilization is observed as a result of the compromise between these two opposite effects.

Introduction

A microemulsion is a thermodynamically stable isotropic dispersion of two immiscible liquids consisting of microdomains of one or both liquids stabilized by the interfacial film of surface-active molecules.[1] Since their discovery, microemulsions have been subjected to numerous theoretical and experimental studies. The microstructure of such microemulsions has been described as droplets of water (or oil) dispersed in a continuous phase of oil (or water) in a certain composition range.[2-5] On the applied front, microemulsions are of interest in enhanced oil recovery, cutting oils, pharmaceutics, cosmetics etc. An important property of a microemulsion is its solubilization capacity for water or oil as microdroplets dispersed in the

* To whom all correspondence should be addressed.

(1) Leung, R.; Hou, M. J.; Manohar, C.; Shah, D. O.; Chun, P. W. In *Macro- and Microemulsions*; Shah, D. O., Ed.; American Chemical Society: Washington, D.C., 1985; p 272.
(2) Dvolaitzky, M.; Guoyt, M.; Lagues, M.; Le Pesant, J. P.; Ober, R.; Sauterey, C.; Taupin, C. *J. Chem. Phys.* **1978**, *69*, 3279.
(3) Auvray, L.; Cotton, J. P.; Ober, R.; Taupin, C. *J. Phys.* (*Les Ulis, Fr.*) **1984**, *45*, 913.
(4) Gulari, E.; Bedwell, B.; Alkhafaji, S. *J. Colloid Interface Sci.* **1980**, *77*, 202.
(5) Zularf, M.; Eicke, H.-F. *J. Phys. Chem.* **1979**, *83*, 480.

0743-7463/87/2403-1086$01.50/0

continuous phase. In this paper, the discussion will be confined to the solubilization of water in w/o microemulsions.

It has been shown that the solubilization of water in microemulsions is strikingly influenced by the chemical structure of the oil and cosurfactant used. For instance, Bansal et al.[6] have shown that there exists a preferred oil chain length which solubilizes more water for a specific surfactant/alcohol pair than others. Johnson and Shah,[7] in formulating alcohol-free microemulsions with a nonionic surfactant as a cosurfactant, found that solubilization of water reached a maximum at a certain value of the surfactant/cosurfactant (AOT/Span-20) ratio. Also, Leong and Candau,[8] using acrylamide as cosurfactant, reported that maximum solubilization was found at a certain concentration of acrylamide.

Although no explanation was given for the last two reports, the concept of "chain length compatibility" has been proposed by Bansal et al. to interpret their results.

From a theoretical consideration, the solubilization capacity of water is geometrically related to the radius of droplets of microemulsions, which is then thermodynamically related to the stability of microemulsions. The basic thermodynamic treatment on the stability of microemulsions has been initiated by Ruckenstein and co-workers.[9-11] In general, the free energy of a microemulsion is primarily decided by the entropic contribution of the dispersion of the droplets in the continuous phase, the interfacial contribution (including the curvature effect), and the interaction between droplets.[9-14] Among the above considerations, the curvature of the interface and the interaction between droplets are strongly influenced by the molecular structures of the interfacial layer and the continuous phase.[15-17] In this study, we started by examining the effects of the curvature effect and the attractive interaction on the stability of microemulsion systems and on the equilibrium radius of droplets at the saturation of solubilization. Then, the influence of the molecular strucure of the components on the curvature of the interface and the attractive interaction between droplets was discussed in relation to the solubilization capacity of water in microemulsions. A plausible model is presented to interpret the solubilization behavior and the maximum solubilization mentioned above. Finally, an experimental study was systematically carried out to support the validity of the model.

Experimental Section

AOT (sodium bis(2-ethylhexyl) sulfosuccinate) of purity 99% sodium was purchased from Sigma; hexane, heptane decane, tridecane, hexadecane, benzene, and toluene were of 99 mol % purity, purchased from Fisher. 1-Propanol, 1-pentanol, 1-hexanol, 1-heptanol, 1-octanol, 1-nonanol, and 1-dodecanol were also 99 mol % pure, purchased from Sigma. Span 20, span 40, and span 60 were obtained from ICI Americas Inc. The above reagents were used without further purification. Acrylamide was of reagent grade, purchased from Fisher. Acrylamide was recrystallized twice before using. Sodium chloride was of certified ACS grade, from Fisher, and was used without further purification.

AOT solution (25%) was prepared with a different oil as the continuous phase. The appropriate amount of cosurfactant was then added. All samples were vigorously stirred for 1 h before measurement. The solubilization capacity of water was measured by titrating water directly into the sample under vigorous stirring. The onset of permanent turbidity or birefringence was taken to indicate the saturation of solubilization. The birefringence was checked with the aid of polarized plates. Phase behavior was observed with the help of either the oil-soluble dye Sudan IV or the water-soluble dye methylene blue after the saturated systems were placed at room temperature for 30 days.

Results and Discussion

Theoretical Considerations. 1. Solubilization Capacity and Radius of Microemulsion Droplets. For a microemulsion system composed of n identical spherical droplets, one can write

$$n_s\Sigma = n4\pi R^2$$

$$n_s v_s + n_w v_w = n(4\pi R^3)/3$$

where n_s and v_s are the number and the individual volume of the surfactant molecule, n_w and v_w are the number and the volume of a water molecule, and R and Σ are the external radius and the external interfacial area occupied by each surfactant molecule. From the above equations, it follows that

$$n_w/n_s = \Sigma R/(3v_w) - v_s/v_w \quad (1)$$

In general, Σ is a very weak function of radius for reasonably large R and tends toward a well-defined limited value on approaching saturation of solubilization.[15,18,19] Thus, n_w/n_s is proportional to the radius of microemulsion droplets, as has been experimentally observed.[20-22] If the solubilization capacity is defined as

$$(n_w/n_s)^* = \Sigma^* R^*/(3v_w) - v_s/v_w \quad (2)$$

the solubilization capacity is then proportional to the radius of the microemulsion droplets at saturation, R^*. Here the superscript * represents the value obtained at saturation (the point phase separation is first observed). Therefor, the stability of microemulsion against phase separation has to be examined in order to determine the value of R^*. At least two types of phase separation have been reported in the literature,[12,16-17,23-31] as described in the following section.

(6) Bansal, V. K.; Shah, D. O.; O'Connell, J. P. *J. Colloid Interface Sci.* **1980**, *75*, 462.
(7) Johnson, K.; Shah, D. O. *J. Colloid Interface Sci.* **1985**, *107*, 269.
(8) Leong, Y. S.; Candau, F.; Pouyet, G.; Candau, S. *J. Colloid Interface Sci.* **1984**, *101*, 167.
(9) Ruckenstein, E.; Chi, J. C. *J. Chem. Soc., Faraday Trans. 2* **1975**, *71*, 1690.
(10) Ruckenstein, E. *Chem. Phys. Lett.* **1978**, *57*, 517.
(11) Ruckenstein, E.; Krishnan, R. *J. Colloid Interface Sci.* **1979**, *71*, 321.
(12) Miller, C. A.; Neogi, P. *AIChE J.* **1980**, *26*, 217.
(13) Huh, C. *J. Colloid Interface Sci.* **1979**, *71*, 408.
(14) Miller, C. A.; Hwan, R. W.; Benton, W. J.; Fort, T., Jr. *J. Colloid Interface Sci.* **1977**, *61*, 554.
(15) De Gennes, P. G.; Taupin, C. *J. Chem. Phys.* **1984**, *86*, 2294.
(16) Mukherjee, S.; Miller, C. A.; Fort, T., Jr. *J. Colloid Interface Sci.* **1983**, *91*, 223.
(17) Cazabat, M.; Langevin, D.; Mennier, J.; Abillon, O.; Chatenay, D. In *Macro- and Microemulsions*; Shah, D. O., Ed.; American Chemical Society: Washington, D.C., 1985; p 75.
(18) Eicke, H.-F.; Rehak, J. *Helv. Chim. Acta* **1976**, *59*, 2883.
(19) Maitra, A. *J. Phys. Chem.* **1984**, *88*, 5122.
(20) Mathews, M. B.; Hirschhorn, E. *J. Colloid Interface Sci.* **1979**, *68*, 22.
(21) Fletcher, F. D. I.; Robinson, B. H.; Barrera, F. B.; Oakenfull, D. G. In *Microemulsions*; Robb, I. D., Ed.; Plenum: New York, 1982; p 221.
(22) Nicholson, J. D.; Clark, J. H. R. In *Surfactants in Solution*; Mittal, K. L., Lindman, B., Eds.; Plenum: New York, 1984; p 1663.
(23) Huh, C. Symposium on Enhanced Oil Recovery, Tulsa, OK, 1982.
(24) Safran, S. A.; Turkevich, L. A. *Phys. Rev. Lett.* **1983**, *50*, 1930.
(25) Jouffroy, J.; Levinson, P.; de Gennes, P. G. *J. Phys. (Les Ulis, Fr.)* **1982**, *43*, 1241.
(26) Adamson, A. W. *J. Colloid Interface Sci.* **1969**, *29*, 261.
(27) Huh, C. *J. Colloid Interface Sci.* **1984**, *97*, 201.
(28) Cazabat, A. M.; Langevin, D.; Meunier, J.; Pouchelon, A. *J. Phys. Lett.* **1982**, *43*, 89.
(29) Chatenary, D.; Abillon, O.; Meunier, J.; Langevin, D.; Cazabat, M. In *Macro- and Microemulsions*; Shah, D. O., Ed.; American Chemical Society: Washington, D.C., 1985; p 119.
(30) Cazabat, A. M.; Langevin, D.; Meunier, J.; Pouchelon, A. *Adv. Colloid Interface Sci.* **1982**, *16*, 175.
(31) Roux, D.; Bellocq, A. M. In *Macro- and Microemulsions*; Shah, D. O., Ed.; American Chemical Society: Washington, D.C., 1985; p 105.

2. Phase Separation Induced by the Curvature Effect. The important effect of curvature has been recognized for years in the equilibrium between a water/oil microemulsion and excess water.[12-13,16,23-26] The curvature effect arises because interaction between adjacent molecules is not uniform across the interfacial layer; i.e., adjacent polar heads interact differently from adjacent hydrocarbon chains. The result is an interfacial bending streess which can cause a flat film to curve. At an equilibrium condition with negligible interfacial tension, an interface would assume an optimal curvature, $1/R^0$, known as spontaneous curvature.[15] The curvature effect thus reflects the tendency of the surfactant interface to bend locally toward either the oil or water region through the radius of spontaneous curvature.[16] For many problems involving the fluid/fluid interface, the curvature effect may represent only a very minor correction, and the interfacial energy is dominated by the tension γ of the flat interface. However, when we are dealing with an interface where $\gamma \rightarrow 0$, such as the one in microemulsion, the curvature effect becomes significant. For a single phase of identical spherical droplets, the interfacial free energy per unit volume f_i can be written as[15,24,32-34]

$$f_i = (3\phi/R)[\gamma + 2K(1/R - 1/R^0)^2] \quad (3)$$

where R is the actual radius of the droplets, R^0 the radius of the spontaneous curvature of droplets, ϕ the volume fraction of droplets, and K a parameter with the dimension of energy whose value is in the order of 0.1 eV.[15,24,32] K is sometimes referred to as the rigidity constant of the interface.

As pointed out by Safran and Turkevich,[24] when the curvature effect is dominant phase separation occurs whenever R approaches R^0. The physical origin of this phase separation exists in the interfacial energy being minimized for $R \cong R^0$. The above reasoning can be summarized mathematically as follows. If a microemulsion system is regarded as identical spheres dispersed in a continuous oil, the total free energy per unit volume of system can be written as

$$f = \Delta g_m + f_i \quad (4)$$

where Δg_m is the contribution from both the entropy of mixing the spheres with continuous oil and the interaction among spheres. The phase equilibrium condition of the microemulsion phase and the excess water phase requires[11]

$$(\partial f/\partial R)_\phi = (\partial f/\partial \phi)_R = 0 \quad (5)$$

The radius of droplets at the point of phase separation induced by the curvature effect, $R^*_{me/w}$, can be determined through the evaluation of eq 5. Note that the subscript me/w indicates a microemulsion phase is in equilibrium with an excess water phase. It has been shown[16] that the first term in eq 4 only gives a small correction to the droplet radius in the case of the equilibrium between a water/oil microemulsion and excess water. Considering the extreme case of K being very large, so that $f_i \gg g_m$,[35] then eq 5 is simplified as

$$(\partial f_i/\partial R)_\phi = (\partial f_i/\partial \phi)_R = 0 \quad (6)$$

Substituting (3) into (6), we obtained the following equivalent expressions:

$$\gamma^* \approx 0 \quad \text{and} \quad R^*_{me/w} \approx R^0 \quad (7)$$

The implication of the above equations can be easily understood. For a small volume fraction of water, droplets with radius $R < R^0$ are formed. The radius of droplets grows as water is added. When R reaches R^0, the curvature energy can be minimized by expelling the excess water into a separate phase so that all droplets are constrained to an optimum size, R^0.

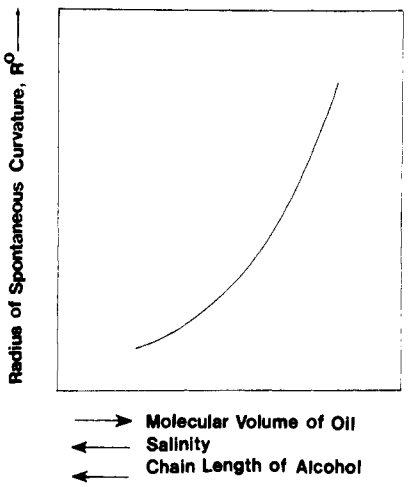

Figure 1. Schematic illustration of the effect of the variation of the molecular volume of oil, salinity, and chain length of alcohol on the radius of spontaneous curvature. Note that the arrows point to the direction of the increase in the value of the variable.

The radius of spontaneous curvature, R^0, can be estimated from more detailed thermodynamic consideration of this equilibrium. Recently, Mukherjee, Miller, and Fort[16] and Jeng and Miller[36] have calculated the interfacial energy of microemulsion droplets by using a lattice model for the hydrocarbon chain region and a hard disk for the polar head of surfactants. By neglecting the free energy of mixing of the droplets with the continuous phase and the free energy of interaction between droplets, they minimized the free energy of the interfacial layer to obtain the radius of spontaneous curvatur of droplets (or the natural radius of droplets). Their results remarkably showed the influence of the chemical structure of the components on the radius of spontaneous curvature of droplets. In water/oil microemulsion, it was found that the radius of spontaneous curvature decreases, and hence the solubilization capacity of water decreases, as the chain length of oil decreases, the chain length of cosurfactant increases, or the size of the polar head decreases. Although their model was developed only for nonionic surfactants, they qualitatively interpreted the effect of salinity by considering the effective area of the polar head, which is determined by the thickness of the electrical double layer. Huh[23] also considered the equilibrium of microemulsion that coexists with excess fluid. His results concluded that the solubilization capacity of water in w/o microemulsion decreased with increasing salinity or decreasing molecular volume of oil. Therefore, for the systems where the phase instability is induced by the curvature effect leading to the coexistence of microemulsion phase and excess water, we can summarize the above discussion with Figure 1.

Unfortunately, the above studies were restricted to the systems where the curvature effect dominates the behavior and cannot completely explain the solubilization behavior of some systems that are also strongly influenced by the attractive interaction between droplets.

3. Phase Separation Induced by Attractive Interaction among Microemulsion Droplets. Experimen-

(32) Safran, S. A. *J. Chem. Phys.* **1983**, *78*, 2073.
(33) Helfrich, W. *Z. Naturforsch.* **1973**, *28*, 693.
(34) Ruckenstein, E. *J. Colloid Interface Sci.* **1986**, *114*, 173.
(35) If we take $\gamma \approx 10^{-2}$ dyn/cm and $K \approx 0.1$ eV and arbitrarily set $\phi \approx 0.1$–0.5, $R \approx 50$ Å, and $R^0 \approx 60$–70 Å, from eq 3 and 13, we can estimate that $f_i \approx 10^{-24}$–10^{-26} J/Å^3 and $\Delta g_m \approx 10^{-25}$–$10^{-27}$ J/Å^3.
(36) Jeng, J.-F.; Miller, C. A. In *Surfactants in Solution*; Mittal, K. L., Lindman, B., Eds.; Plenum: New York, 1984; p 1829.

tally, phase separation has also been observed in several microemulsion systems to associate with a critical point, with correlation length appropriate for a binary mixtur.[30-31,37] Such phase separation usually leads to the coexistence of two microemulsion phases having the same continuous component.[24,27-31] Furthermore, measurement of second virial coefficients in the single-phase region indicated that those systems possessing a critical point are characterized by large attractive interaction between microemulsion droplets.[17,30-31,38]

If we considered a microemulsion as a binary mixture of rigid spheres in a dispersing medium (continuous oil), the phase instability can be examined through its free energy of mixing, Δg_m. Vrij et al.[39] have shown that the light scattering of microemulsions can be well interpreted by a hard-sphere potential, U_{hs}, with a small perturbation of attraction, U_a. That is, the interaction potential $U = U_{hs} + U_a$. Therefore, the osmotic pressure, Π, of microemulsion can be written as

$$\Pi = \Pi_{hs} + \Pi_a \quad (8)$$

where Π_{hs} is the osmotic pressure of a hard sphere and Π_a the perturbation in osmotic pressure from attractive contribution. Π_{hs} can be accurately described by the Percus–Yevick[40]–Carnahan–Starling[41] approximation, i.e.

$$\Pi_{hs} = kT(\phi_{hs}/v_{hs})(1 + \phi_{hs} + \phi_{hs}^2 - \phi_{hs}^3)/(1 - \phi_{hs})^3 \quad (9)$$

where v_{hs} is the volume of a hard sphere, ϕ_{hs} the volume fraction of hard spheres, k the Boltzmann constant, and T the absolute temperature. Π_a can be written as[42]

$$\Pi_a = (\phi_{hs}/v_{hs})^2 2\pi \int_0^\infty U_a(r) g_{hs}(r) r^2 \, dr + \text{higher order terms}$$

where r is the separation distance between the center of two spheres and $g_{hs}(r)$ the radial distribution function of hard spheres, i.e.

$$g_{hs}(r) = \exp[-U_{hs}(r)/(kT)]$$

For simplicity, we dropped out higher order terms, thus

$$\Pi_a = (\phi_{hs}/v_{hs})^2 2\pi \int_\sigma^\infty U_a(r) r^2 \, dr$$

$$= (kT/v_{hs})(A\phi_{hs}^2/2) \quad (10)$$

where σ is the diameter of a hard sphere and

$$A = 4\pi/(kTv_{hs}) \int_\sigma^\infty U_a(r) r^2 \, dr \quad (11)$$

Therefore, from eq 8, 9, and 10, we have

$$\Pi = (kT/v_{hs}) \times [\phi_{hs}(1 + \phi_{hs} + \phi_{hs}^2 - \phi_{hs}^3)/(1 - \phi_{hs})^3 + A\phi_{hs}^2/2] \quad (12)$$

Following an approach similar to the one presented by Overbeek,[43] we have derived from eq 12 the formula of the free energy of mixing for a unit volume (see Appendix A)

$$\Delta g_m/(kT) = (\phi_{hs}/v_{hs})[\ln \phi_{hs} + \phi_{hs}(4 - 3\phi_{hs})/(1 - \phi_{hs})^2 - 1 + \ln (v_o/v_{hs}) + A\phi_{hs}/2] \quad (13)$$

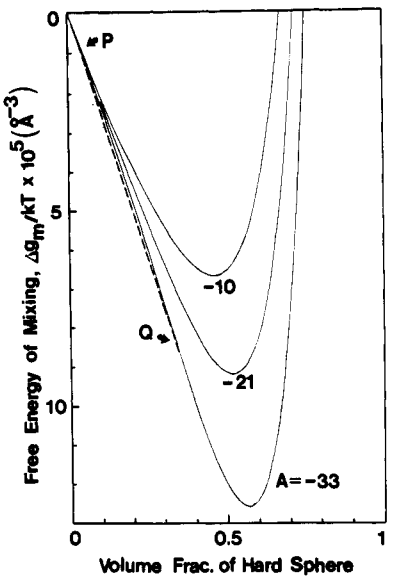

Figure 2. Variation of Δg_m as a function of the volume fraction of hard spheres at different strengths of attraction between spheres. The radius was arbitrarily set at 50 Å in all calculations, because the variation of this value can change the absolute value of Δg_m only without altering the shape of curve, if the value of A is fixed. The lowest curve showed the phase instability induced by the strong attraction.

where the dimensionless parameter A, defined in eq 11, represents the strength of the attractive interaction between spheres and v_o the molecular volume of oil.

The stability of the binary mixture (microemulsion) can be examined by evaluating the free energy of mixing as a function of volume fraction at different strengths of attraction. From eq 13, a critical attraction strength, $A_c = -21$, was obtained by fulfilling the critical condition for binary mixing, i.e.

$$[\partial^2 \Delta g_m/\partial \phi_{hs}^2]_{A=A_c} = [\partial^3 \Delta g_m/\partial \phi_{hs}^3]_{A=A_c} = 0 \quad (14)$$

From Figure 2, we can see that the Δg_m vs ϕ_{hs} curve exhibits convex downward behavior over the entire composition range if A is greater than A_c. Thus, the system can always stay as a stable single phase until the free energy became a positive value when the hard sphere repulsion dominated due to the high concentration of spheres present in the solution. As A approached A_c, an inflection point was found at $\phi_{hs} = \phi_c = 0.13$, where the systems started to become unstable. Once the value of A became smaller than $A_c = -21$, the Δg_m vs ϕ_{hs} curve exhibited slight convex upward behavior over the volume fraction range between P and Q. It can be seen that over this volume fraction range P–Q the dashed line was always lower than solid line; i.e., the system's free energy was minimized if two phases of composition P and Q were present instead of a single phase of any intermediate composition. Therefore, the system became unstable against the separation into two phases of spheres with the same continuous component, oil, as indicated by P and Q. Note that the radius of spheres was kept constant in the above evaluation for each value of A throughout the whole composition range. Thus, the growth of spheres, as would be expected in the solubilization process, did not enter the evaluation in each Δg_m vs ϕ_{hs} curve. Instead, the growth of spheres is considered through the increase of the value of A.

Since A is a function of $U_a(r)$ (see eq 11), we would expect that the value of A depends on the nature and composition of surfactant, cosurfactant, and oil, as well as the radius of spheres, as experimentally observed by many researchers.[29-31,38-39,44-46] For a given microemulsion system

(37) Huang, J. S.; Kim, M. W. *Phys. Rev. Lett.* **1981**, *47*, 1462.
(38) Forche, G.; Bellocq, A. M.; Brunetti, S. *J. Colloid Interface Sci.* **1982**, *88*, 302.
(39) Calje, A.; Agterof, W.; Vrij, A. In *Micellization, Solubilization and Microemulsion*; Mittal, K. L., Ed.; Plenum: New York, 1977; p 780.
(40) Percus, J. K.; Yevick, G. J. *Phys. Rev.* **1958**, *110*, 1.
(41) Carnahan, N. F.; Starling, K. E. *J. Chem. Phys.* **1969**, *51*, 635.
(42) Barker, J. A.; Henderson, D. *J. Chem. Phys.* **1967**, *47*, 2856.
(43) Overbeek, J. Th. G. *Faraday Discuss. Chem. Soc.* **1978**, *65*, 7.

at a given temperature, it is clear that all the influencing factors just mentioned above are fixed except the radius of spheres during the solubilization process. Experimentally, it has been shown that the increase of the radius microemulsion droplets increased the strength of attraction,[29,45,47] that is, decreased the value of A. If we imagine the solubilization process as a combination of the growth of spheres and the mixing of these spheres with continuous oil, then in the initial stage of solubilization the spheres are small and, hence, stable for binary mixing. However, as the amount of water solubilized increases, the spheres will grow as indicated by eq 1. At a certain point, the radius of these spheres will reach a critical value, R^c, so that $A = A_c$; thus the binary mixture of these spheres and continuous oil starts to become unstable and separates into two phases of spheres with the same continuous component, oil. Therefore, the solubilization capacity of microemulsions will be limited by the value of $R^*_{me/me} = R^c$ in this case, whre the subscript me/me stands for the phase equilibrium between two microemulsion phases.

To further analyze the effects of other important structural factors on the variation of R^c, one needs to understand the origin of the attraction among microemulsion droplets, so that more structured interaction potential can be constructed. Calje et al.[39] have proposed that this attraction is the result of the difference in the molecular composition between droplets and the continuous medium. However, the application of Hamaker's work for the dispersion of homogeneous spheres in solvent to water/oil microemulsions by Calje et al.[39] led to a very weak attraction when realistic values were assumed for the Hamaker constant. In order to explain this inconsistency, Calje et al.[39] suggested that the interpenetration of microemulsion droplets should be taken into account. Such modification has been carried out by Lemaire, Bothorel, and Roux in their recent derivation of a mean field intermicellar potential.[44,45] A detailed calculation by these authors has shown that the most important contribution to the attractive interaction occurred in the overlapping region. Assuming that the potential is short range relative to the volume considered, this potential is further simplified by Roux, Bellocq, and Bothorel[46] as

$$U(r) = 0 \quad r > 2R$$

$$U(r) = -kT\Delta\rho(2R - r)^2(2R + r/2)/6 \qquad 2R - \xi < r < 2R \quad (15)$$

$$U(r) = \infty \quad r < 2R - \xi$$

where r is the separation distance between the centers of two spheres. ξ is a parameter phenomenologically used to characterize the penetrable length of the interfacial layer during interpenetration of droplets. One can expect that ξ will be smaller, if the interfacial layer is more rigid. Such rigidity can be achieved through a more compact packing in the interface by using longer alcohol chains or increasing salinity (or decreasing head area of the polar group). $\Delta\rho$ is a constant depending on the compositions of the interface and the continuous phase. As shown by Roux et al.,[46] the parameter $\Delta\rho$ appears to be very sensitive to the type of oil molecule used and is strongly correlated to the molecular volume of oil. An increase of the molecular volume of oil corresponds to an increase of the value of $\Delta\rho$ and an increase of the interaction potential. According to Lemaire et al.,[44] the attractive potential is very sensitive and increases with the difference between the atomic densities in the continuous phase and in the penetrable part of the interfacial layer. In eq 15, $\Delta\rho$ is actually equivalent to the difference of densities just mentioned. One would expect this difference to increase with the difficulty for oil to penetrate the interfacial layer. This difficulty is obviously related to the molecular volume of oils used. We also noted that Pincus and Safran[48] have shown that the attraction theoretically can be induced by the perturbation of surfactant concentration in bulk phase when microemulsion droplets are close to one another. Their calculation showed that the attractive interaction is proportional to A and varied with the radius of droplets. However, no detail has been given for the dependence of interaction on other structural factors. Experimentally, it has been shown that the increase of attraction is associated with an increasing penetrable length of interfacial region as evidenced from an increasing difference between the hard-sphere radius and the hydrodynamic radius.[2,17,45,49-51] It has also been found that the increase of the chain length of the oil used increased the attraction among droplets.[29,45-47]

It is clear that R^c can be quantitatively determined once a suitable potential function is given in an explicit form. Since no suitable potential function has been proposed, we have implicitly expressed the potential in a more generalized form so that the effects of the molecular structure of the interface and continuous phase on R^c can be qualitatively illustrated. That is

$$A = A(R,T,\xi,\Delta\rho) \quad (16)$$

The inclusion of ξ and $\Delta\rho$ into eq 16 is necessary from the above discussion. It is easy to show (see Appendix B) that

$$(\partial R^c/\partial\xi)_{A=A_c} < 0 \quad (17)$$

$$(\partial R^c/\partial\Delta\rho)_{A=A_c} < 0 \quad (18)$$

That is, the critical droplet radius R^c increases as one decreases the penetrable length of the interfacial layer during the collision or decreases the molecular volume of the oil used so that $\Delta\rho$ decreases. Actually, A can be expressed in a more general form based on experimental facts:

$$A = A(R,T,x_1,x_2,x_3,x_4,\text{etc.})$$

where x_1 is the molecular volume of oil used, x_2 the chain length of alcohol used, x_3 the salinity, and x_4, etc., other factors that may influence the attractive interaction. Again, it is easy to show that

$$(\partial R^c/\partial x_1)_{A=A_c} < 0 \quad (19)$$

$$(\partial R^c/\partial x_2)_{A=A_c} > 0 \quad (20)$$

$$(\partial R^c/\partial x_3)_{A=A_c} > 0 \quad (21)$$

The implication of inequality in eq 19–21 is schematically shown in Figure 3.

4. Solubilization Capacity and Maximum Solubilization. In the last two sections, two radii have been

(44) Lemaire, B.; Bothorel, P.; Roux, D. *J. Phys. Chem.* **1983**, *87*, 1023.
(45) Brunetti, S.; Roux, D.; Bellocq, A. M.; Bothorel, P. *J. Phys. Chem.* **1983**, *87*, 1028.
(46) Roux, D.; Bellocq, A. M.; Bothorel, P. In *Surfactants in Solution*; Mittal, K. L., Lindman, B., Eds.; Plenum: New York, 1984; p 1843.
(47) Hou, M. J.; Shah, D. O., in preparation.
(48) Pincus, P. A.; Safran, S. A. *J. Chem. Phys.* **1987**, *86*, 1645.
(49) Ober, R.; Taupin, C. *J. Phys. Chem.* **1980**, *84*, 2418.
(50) Cazabat, A. M.; Langevin, D. *J. Chem. Phys.* **1981**, *74*, 3148.
(51) Brouwer, W. M.; Nieuwenhuis, E. A.; Kops-Werkoven, M. M. *J. Colloid Interface Sci.* **1983**, *92*, 57.

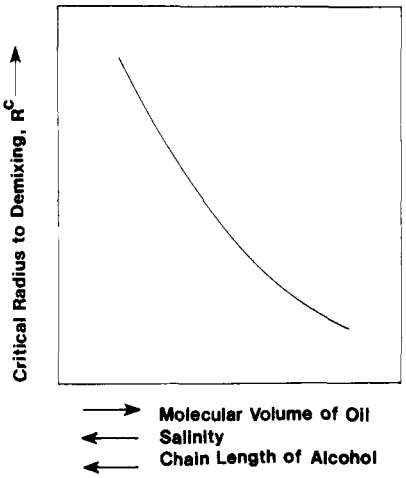

Figure 3. Schematic illustration of the effect on R^c caused by the variation of the molecular volume of oil, salinity, and chain length of alcohol. Note that the trend of the variation of R^c is exactly opposite to that of R^0 as shown in Figure 1.

defined, $R^*_{me/w}$ and $R^*_{me/me}$. Considering the equilibrium between microemulsion phase and excess water, a saturated radius $R^*_{me/w}$ can be determined by

$$(\partial f/\partial R)_\phi = 0$$

$$(\partial f/\partial \phi)_R = 0$$

With the assumptions made earlier, we have shown that $R^*_{me/w}$ is approximately R^0. On the other hand, another saturated radius $R^*_{me/me}$ can be determined by fulfilling the critical condition of a binary mixture, i.e.

$$(\partial^2 \Delta g_m/\partial \phi_{hs})_{R=R_c} = 0$$

$$(\partial^3 \Delta g_m/\partial \phi_{hs})_{R=R_c} = 0$$

Therefore, for a given microemulsion system, the solubilization capacity will be determined by

$$R^* = \min(R^*_{me/w}, R^*_{me/me})$$

Hence, the solubilization capacity of water in water/oil microemulsion will be limited by either R^c or R^0, depending on the relative magnitude of R^c and R^0.

We can now explain the maximum solubilization as mentioned in the introduction. For a system with a very rigid interface, the values of $\Delta\rho$ and ξ are very small. The effect of the interaction among droplets may be neglected compared to the curvature effect, and hence one would expect the solubilization to be limited by the radius of spontaneous curvature. In this case, solubilization can be improved by decreasing the spontaneous curvature of the interfacial film by making the interfacial layer more "fluid" (e.g., using a cosurfactant with shorter chain length, increasing the amount of cosurfactant, decreasing the salinity, or replacing the continuous component with larger oil molecules). However, by doing so, we also increased the values of ξ and $\Delta\rho$ and thus increased the interaction strength among droplets. Hence, such improvement will be limited as the increasing radius, R^0, of the spontaneous curvature meets the decreasing critical radius of droplet, R^c. After that, any increase in ξ or $\Delta\rho$ will decrease the solubilization capacity by further decreasing the critical droplet radius. Hence, one would expect the existence of maximum solubilization of water at a specific value of a component variable when attempting to improve the solubilization through a systematic change of the chain length or concentration of components. Indeed, this argument is consistently supported by our experimental results, as discussed in the next section.

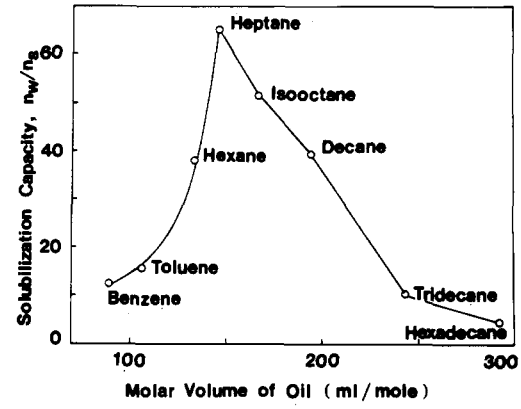

Figure 4. Effect of the molecular volume of oil on the solubilization capacity of microemulsion AOT–oil–water at room temperature. The oil used was shown along each data point.

Interpretation of Experimental Results

Figure 4 showed the effect of the molecular volume of oil on the solubilization of water in water/oil microemulsions. For the systems with small oil molecules, where the penetration of oil into the interfacial layer is large and the attractive strength is small,[29,45-47] the large penetration of oil, meanwhile, favors the greater spontaneous curvature, so R^0 is small. Thus, the solubilization capacity of water in such systems tends to be limited by the value of the radius of spontaneous curvature, as indicated by eq 7. The phase separation in the systems is induced by the curvature effect whenever the value of the radius of droplets approaches R^0. We can further check the behavior of the phase separation of these systems at the saturation of solubilization. When the oil-soluble dye Sudan IV was added to the systems containing benzene, toluene, or *n*-hexane after phase separation, the red color quickly dissolved in the top phase, while a small volume of excess fluid settled at the bottom remained clear and colorless. The above observation indicated the equilibrium phases are a water/oil microemulsion phase and the excess water phase. As we can see, the replacement of the continuous component with larger oil molecules increased the solubilization capacity in the range of 50–150 mL/mol of molar volume of oil. As the molar volume of the oil is increased further, the large attractive interaction among droplets plays the major role in the decrease of the solubilization capacity of water by limiting the actual radius to smaller values than the critical droplet radius R^c. The observation of the behavior of phase separation is again consistent with the statement we just made. When Sudan IV was added to the systems containing *n*-decane, *n*-tridecane, or *n*-hexadecane after phase separation, a red color quickly developed in both phases, indicating that both phases are oil-continuous, as expected. When the water-soluble dye methylene blue was added, we saw the bottom phase quickly turn blue, while the upper phase remained colorless, implying that only a negligible amount of water is present in the upper phase. It is interesting to point out that eq 13 always predicts a negligible amount of water in the water-lean phase, as shown by P in Figure 2.

The effect of salinity on solubilization is shown in Figure 5. It has been shown that the increase of salinity in water/oil microemulsions will decrease the attractive interaction among droplets by making the interfacial layer more rigid due to closer packing of polar groups,[29,49] so that the degree of interpenetration of droplets is reduced during collision. As evidenced in Figure 4, for the system AOT–*n*-tridecane–water, the solubilization of water is limited

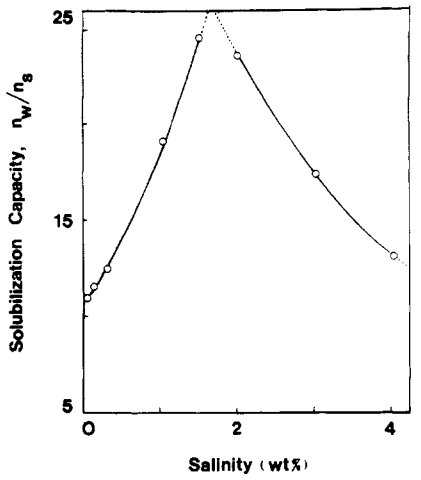

Figure 5. Solubilization of brines of different salinity in microemulsion AOT–tridecane–brine at room temperature.

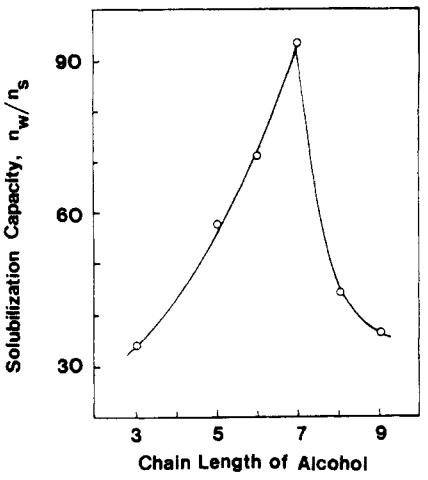

Figure 6. Effect of the chain length of alcohol on the solubilization capacity of water at room temperature. The system studied is AOT–decane–water–alcohol, and the alcohol concentration was fixed at [alcohol]/[AOT] = 0.5 mol/mol for all the alcohols used.

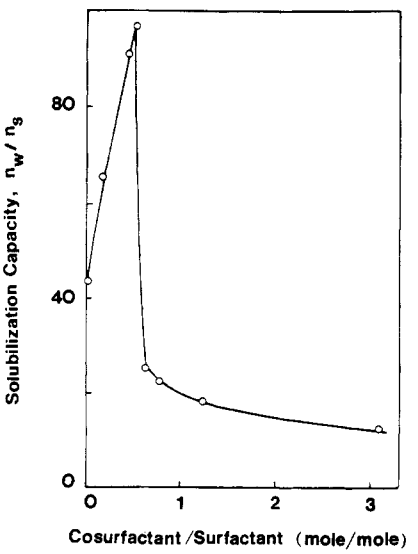

Figure 7. Effect of alcohol concentration on the solubilization capacity of water at room temperature. The system studied is AOT–decane–1-heptane–water.

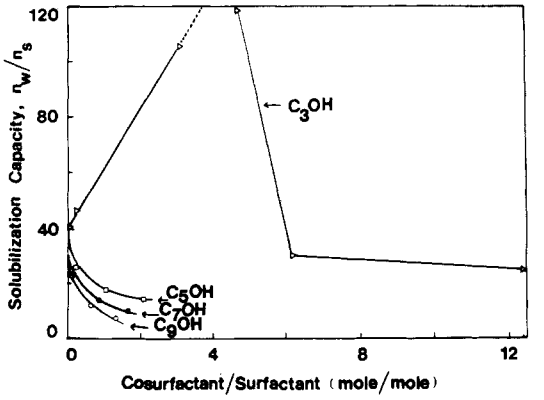

Figure 8. Variation of solubilization capacity of water at room temperature as a function of the concentration of several alcohols. The system studied is AOT–hexane–alcohol(1-propanol, 1-pentanol, 1-heptanol, 1-nonanol).

by the critical droplet radius R^c. For this system, the solubilization capacity increased, as expected, when we increased salinity to 1.5 wt %. However, the increase of salinity also decreases the radius of spontaneous curvature by decreasing the thickness of the electrical double layer around the polar group of surfactants and hence the area per polar group, as pointed out by Mukherjee et al.[16,36] and Huh.[23] Therefore, the solubilization capacity started decreasing with more addition of salt after reaching maximum solubilization. The behavior of the solubilization capacity showed the same trend as one changed the chain length or concentration of alcohols, as shown in Figures 6 and 7. The effect of adding cosurfactant to the interfacial layer is more complicated than the ones we have discussed.

The spontaneous curvature of the interfacial layer depends on the stress in both sides of layer. At equilibrium, balance must exist between the head and the tail stresses. Addition of alcohol to a layer with fixed surfactant concentration will decrease both the head and tail stresses. The change in the head stress is independent of the chain length of alcohol, but decrease of the stress in the tail side is greater for a shorter alcohol chain as it will leave larger cavities between surfactant chains. Hence, as pointed out by Mukherjee et al.,[16] in systems formed with long-chain alcohols where the decrease of stress is greater in the head side one would expect a decrease in the radius of spontaneous curvature and the reverse for systems with short-chain alcohols, where the decrease of stress in the tail side is greater. Our experimental results clearly confirmed this point. As shown in Figure 8, for the system AOT–hexane–water where the solubilization of water is limited by the natural radius of curvature as evidenced in Figure 4, the addition of long-chain alcohols such as 1-pentanol, 1-heptanol, or 1-nonanol decreased the solubilization capacity and the magnitude of reduction increased with the chain length or the concentration of alcohol used. The solubilization capacity of water increased, as expected, with the addition of the short-chain alcohol 1-propanol and reached a maximum, limited by the decreasing critical droplet radius. The effect of added alcohols on the strength of interaction among droplets can be illustrated as follows. For microemulsions of the same droplet size formed with the same oil, at fixed temperature, the attractive interaction is very much determined by the penetrable length during the interpenetration of droplets. Penetrable length can be viewed as the difference between the hydrodynamic radius and the hard-sphere radius of droplets. For the systems formed with single-chain surfactants, the hard-sphere radius has been found to be very close to the sum of the water core radius and the chain length of the alcohol in many cases.[2,50] For water/oil microemulsions formed with AOT, oil, and water, with the richness of oxygen and carbonyl group in AOT, one would

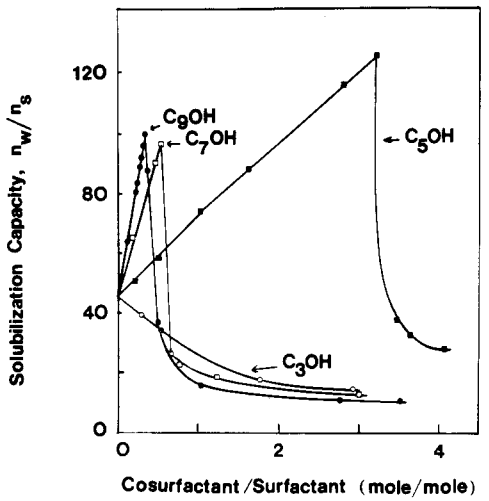

Figure 9. Variation of solubilization capacity of water at room temperature as a function of the concentration of different alcohols. The system studied is AOT–decane–alcohol–water.

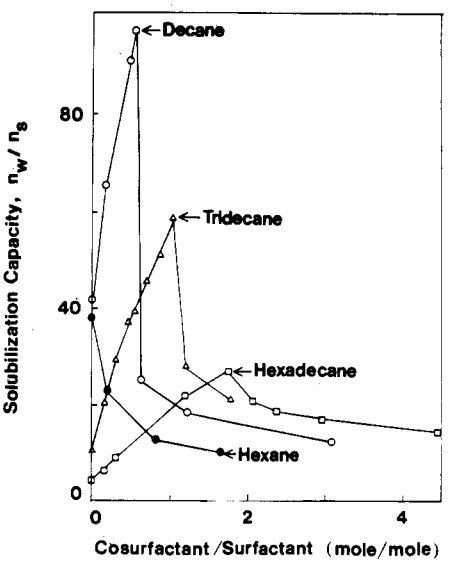

Figure 10. Effect of 1-heptanol concentration on the solubilization capacity of water at room temperature in several microemulsion systems containing different oils. The system studied is AOT–oil(hexane, decane, tridecane, or hexadecane)–1-haptanol–water.

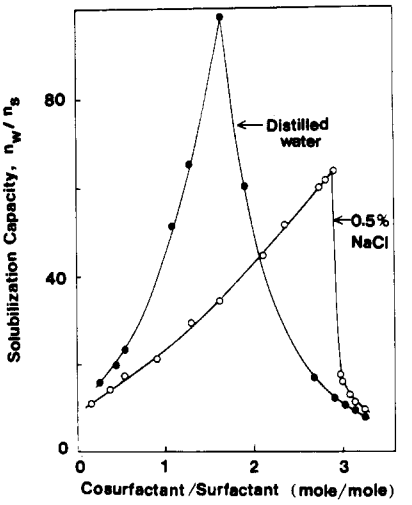

Figure 11. Effect of acrylamide concentration on the solubilization capacity of water or 0.5 wt % brine at room temperature. The system studied is AOT–toluene–acrylamide–water(or brine).

estimate the distance between the water core and the hard-sphere boundary to be the chain length of four to five carbons. For such systems, one expects the increase of penetrable length during collision of droplets when the chain length of the alcohols added is shorter than this length and the reverse when the alcohol chain length is longer than this length. And it is obvious that such effects will increase with the increase of cosurfactant concentration. This argument is, again, supported by our experimental results. As seen in Figure 4, the solubilization capacity of water in the AOT–decane–water system is limited by the critical droplet radius R^c through the interaction among droplets. In Figure 9, it is clearly shown that the solubilization of water in this system was improved with added 1-pentanol, 1-heptanol, or 1-nonanol and the degree of the improvement increased with the increase of the chain length. However, addition of long-chain alcohols also decreases the radius of spontaneous curvature as discussed above. Hence, maximum solubilization was, again, found for each case. The results also consistently showed that the decrease of the radius of spontaneous curvature is greater for longer alcohol chains. Thus, one needs a smaller amount of alcohol to reach the maximum for longer alcohol chains in this system. The addition of 1-propanol to this system, as expected, resulted in the reduction of solubilization as the penetrable length is increased during collision of droplets, leading to the decrease of the critical droplet radius.

Figure 10 illustrates the effect of the combination of alcohol concentration and oil molecular structure. As discussed above, for systems formed with AOT, water, decane, tridecane, or hexadecane, the solubilization is limited by the critical droplet radius R^c through the attractive interaction among droplets. The solubilization was improved when a long-chain alcohol such as 1-heptanol was added to reduce the penetrable length during the interpenetration of droplets. Again, this improvement is limited by the decreasing radius of spontaneous curvature and the maximum solubilization found for each case. The position of the maximum also consistently reflects the effect of the molecular volume of oil. For systems formed with smaller oil molecules, less 1-heptanol is required to increase the spontaneous curvature of the interfacial film to reach maximum solubilization. For the AOT–hexane–water system, where the solubilization of water is already limited by the spontaneous curvature of the interfacial layer, the addition of 1-heptanol, as expected, further decreased the solubilization capacity of water because the natural radius of the droplet is further decreased.

The above discussion is not restricted to the use of only classical cosurfactants such as alcohols. The observations of Johnson et al.[7] and Leong et al.[8] can be interpreted in the same way. Indeed, as shown in Figures 11 and 12, the effects of salinity and cosurfactant chain length are consistent with all the results we have discussed. For the AOT–toluene–water system, where the solubilization is limited by the spontaneous curvature of the film as evidenced in Figure 4, the addition of acrylamide increased the solubilization capacity of water until the decreasing critical droplet radius R^c came to limit this improvement (see Figure 11). The effect of increasing salinity plays an important role in decreasing the radius of spontaneous curvature and increasing the critical droplet radius. In AOT–hexadecane–water, the solubilization of water can be improved by adding nonionic surfactant Span-20 as cosurfactant to decrease the attractive interaction.[47] Again, this improvement is limited by the decreasing radius of spontaneous curvature as the addition of the long-chain nonionic surfactant. The effect of increasing the chain

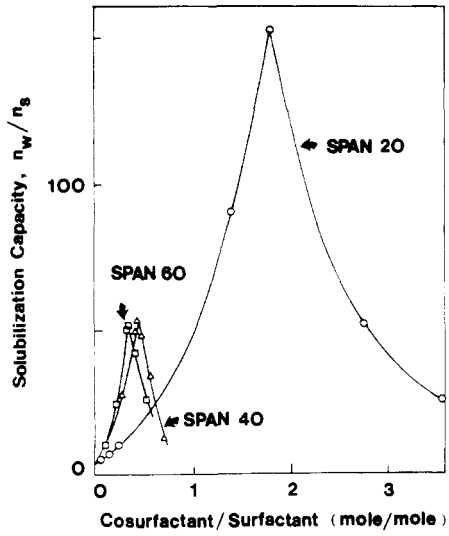

Figure 12. Effect of cosurfactant (nonionic surfactant) concentration on the solubilization capacity of water at room temperature in several microemulsion systems containing different nonionic surfactants. The system studied is AOT–hexadecane–Span-20(Span-40, Span-60)–water.

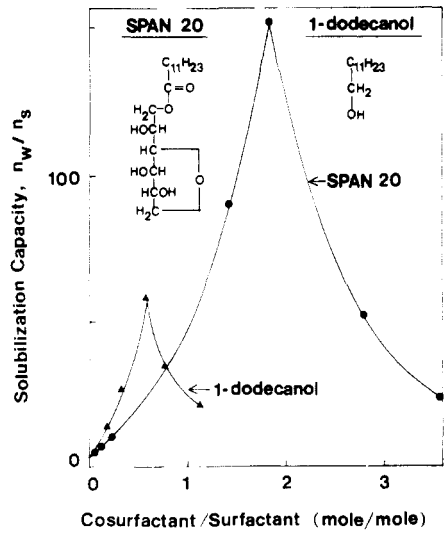

Figure 13. Effect of cosurfactant concentration and the size of the polar group on the solubilization capacity of water at room temperature. The system studied is AOT–hexadecane–Span-20(or 1-dodecanol)–water. The structures of Span-20 and 1-dodecanol were inserted for comparison.

length of the nonionic surfactant again favors the increase of the critical droplet radius and the decrease of the radius of spontaneous curvature. In fact, the suppression of the radius of spontaneous curvature is so overwhelming that the maximum solubilization capacity is much smaller for systems with Span-40 or Span-60 compared with that for the system with Span-20. Figure 13 shows the effect of the size of the polar head of the cosurfactants on the solubilization of water in water/oil microemulsions. It has been shown that the increase of the polar head area increases the attractive interaction among droplets.[45] On the other hand, increasing the size of the polar head undoubtedly will increase the radius of spontaneous curvature.[16,36] This is clearly reflected in Figure 13, where the addition of the cosurfactant with a smaller polar head increased the critical droplet radius and decreased the natural radius more effectively than the addition of the cosurfactant with a larger polar head.

One important piece of evidence, which supports the arguments we have made so far, is the phase behavior of the systems when the limit of solubilization is reached. In most of the systems we studied, two strikingly different patterns of phase separation were observed along the solubilization curve after the samples reached phase equilibrium. Each one corresponds to the samples on one side of the solubilization curve, separated by maximum solubilization. Two clear phases of microemulsion appeared in one side, where we supposed the phase separation was induced by attraction among droplets, while small visible droplets of bulk water in equilibrium with clear microemulsion phase were observed on the other side, where the phase separation was induced by the curvature effect. This observation certainly supports the arguments we have made; namely, the maximum solubilization of water is the result of the compromise between the effects of curvature and of attraction among droplets.

However, for some systems, notably AOT–acrylamide–water(or brine) and AOT-Span-20(or -40, -60)–water, the observed phase behavior is not quite consistent with the above arguments, because of the emergence of a liquid crystalline phase on solubilization saturation. Such an observation was usually found in the systems around the maximum solubilization of each curve. Further study regarding this aspect is certainly required to completely understand the solubilization behavior in this type of system.

Conclusions

The effects of the molecular structure of the interface and continuous phases on the solubilization capacity of water in water/oil microemulsion have been studied from both theoretical considerations and experimental observations.

From the consideration of the stability of microemulsion systems, the growth of microemulsion droplets during the solubilization process has to be limited either by the radius of the spontaneous curvature of the interface, R^0, as the result of the curvature effect or by the critical radius of the droplets, R^c, due to the attractive interaction among the droplets.

For the systems where the solubilization capacity of water is limited by the spontaneous curvature of the layer, the solubilization capacity can be increased by any modification of the molecular structure of either the interface or continuous phase so that the spontaneous curvature of the layer is decreased (i.e., R^0 is increased). For the systems where the solubilization capacity is limited by the critical droplet radius, the reduction of the attractive interaction among droplets (i.e., increase of R^c) increases the solubilization capacity of water.

Both R^0 and R^c are strongly influenced by the variation of the molecular structure of the interface and continuous phase. Any modification of the molecular structure in either phase can have opposite effects on R^0 and on R^c. For example, the increase of the rigidity of the interface decreases R^0 and increases R^c. Use of smaller oil molecules increases R^c and decreases R^0.

The maximum solubilization was observed as one attempted to improve the solubilization by changing the molecular structure of the interface or continuous phase. This maximum solubilization is a result of the compromise between the two opposite effects on the curvature of the interface and the attraction among droplets.

Acknowledgment. We are grateful to the National Science Foundation (Grant No. NSF-CPE 8005851), the donors of the Petroleum Research Fund (Grant No. PRF-14718-ACS), administered by the American Chemical Society, and the ALCOA Foundation for supporting this

research. We thank Professor J. P. O'Connell and Dr. M. Kim for critical review of the manuscript. We also want to thank one of the referees for providing ref 48 in explaining the origin of the attractive interaction in microemulsions.

Appendix A

If we consider a microemulsion as a binary mixture of interacting rigid spheres in a dispersing medium (oil), then ΔG_m, the free energy required to mix n_{hs} identical spheres with n_o solvent (oil) molecules, can be written as

$$\Delta G_m = n_o(\mu_o - \mu_o^{\ominus}) + n_{hs}(\mu_{hs} - \mu_{hs}^{\ominus}) \quad \text{(A1)}$$

where $\mu_i = \partial G/\partial n_i$ is the chemical potential of component i and the superscript $\ominus$ represents the reference state (pure solute and solvent). The osmotic pressure, Π, of the mixture is related to the chemical potentials via

$$\mu_o - \mu_o^{\ominus} = -\Pi v_o \quad \text{(A2)}$$

where v_o is the molecular volume of the oil. In the text, Π has been shown to be

$$\Pi = \frac{kT}{v_{hs}}\left(\frac{\phi_{hs}(1 + \phi_{hs} + \phi_{hs}^2 - \phi_{hs}^3)}{(1 - \phi_{hs})^3} + \frac{A}{2}\phi_{hs}^2\right) \quad \text{(12)}$$

Substituting (12) into (A2) yields

$$\mu_o - \mu_o^{\ominus} = -v_o\frac{kT}{v_{hs}}\left(\frac{\phi_{hs}(1 + \phi_{hs} + \phi_{hs}^2 - \phi_{hs}^3)}{(1 - \phi_{hs})^3} + \frac{A}{2}\phi_{hs}^2\right) \quad \text{(A3)}$$

Applying the Gibbs–Duhem relation, we have

$$d\mu_{hs}/d\mu_o = -(1 - x)/x \quad \text{(A4)}$$

where x is the molar fraction of spheres. Since x is related to ϕ_{hs} by

$$x = (\phi_{hs}/v_{hs})/[\phi_{hs}/v_{hs} + (1 - \phi_{hs})/v_o]$$

(A4) can be rearranged as

$$d\mu_{hs} = -(1 - \phi_{hs})v_{hs}d\mu_o/(\phi_{hs}v_o) \quad \text{(A5)}$$

Substituting (A3) into (A5), we have

$$d\mu_{hs} = kT\frac{(1 - \phi_{hs})}{\phi_{hs}}d\left(\frac{\phi_{hs}(1 + \phi_{hs} + \phi_{hs}^2 - \phi_{hs}^3)}{(1 - \phi_{hs})^3} + A\phi_{hs}^2\right)$$

$$= kT\left\{\left(\frac{1}{\phi_{hs}} + \frac{2}{(1 - \phi_{hs})^2} + \frac{6}{(1 - \phi_{hs})^3} - 1\right)d\phi_{hs} + A(1 - \phi_{hs})d\phi_{hs}\right\} \quad \text{(A6)}$$

Integrating (A6) from $\phi_{hs} \to 0$ to ϕ_{hs} yields

$$\mu_{hs} - \mu_{hs}|_{\phi_{hs}\to 0} = kT\left(\ln \phi_{hs} + \frac{2}{1 - \phi_{hs}} + \frac{3}{(1 - \phi_{hs})^2} - \phi_{hs} + A\left(\phi_{hs} - \frac{\phi_{hs}^2}{2}\right) - \ln \phi_{hs}|_{\phi_{hs}\to 0} - 5\right)$$

Therefore

$$\mu_{hs} - \mu_{hs}^{\ominus} = kT\left(\ln \phi_{hs} + \frac{2}{1 - \phi_{hs}} + \frac{3}{(1 - \phi_{hs})^2} - \phi_{hs} - 5 + \ln (x/\phi_{hs})|_{\phi_{hs}\to 0} + A(\phi_{hs} - \phi_{hs}^2/2)\right) \quad \text{(A7)}$$

Note that

$$(x/\phi_{hs})_{\phi_{hs}\to 0} = v_o/v_{hs} \quad \text{(A8)}$$

Inserting (A8) into (A7) yields

$$\mu_{hs} - \mu_{hs}^{\ominus} = kT\left(\ln \phi_{hs} + \frac{\phi_{hs}(7 - 3\phi_{hs} - \phi_{hs}^2)}{(1 - \phi_{hs})^2} + \ln (v_o/v_{hs}) + A\left(\phi_{hs} - \frac{\phi_{hs}^2}{2}\right)\right) \quad \text{(A9)}$$

Substituting (A3) and (A9) into (A1), we obtain

$$\Delta G_m = -\frac{n_o v_o}{v_{hs}}kT\left(\frac{\phi_{hs}(1 + \phi_{hs} + \phi_{hs}^2 - \phi_{hs}^3)}{(1 - \phi_{hs})^3} + \frac{A}{2}\phi_{hs}^2\right) + n_{hs}kT\left(\ln \phi_{hs} + \frac{\phi_{hs}(7 - 3\phi_{hs} - \phi_{hs}^2)}{(1 - \phi_{hs})^2} + \ln\left(\frac{v_o}{v_{hs}}\right) + A\left(\phi_{hs} - \frac{\phi_{hs}^2}{2}\right)\right) \quad \text{(A10)}$$

Note that the total volume of the system $v_t = n_o v_o + n_{hs}v_{hs}$, so

$$n_o v_o/v_{hs} = n_{hs}(1 - \phi_{hs})/\phi_{hs}$$

Thus, (A10) can be rearranged as

$$\Delta G_m = n_{hs}kT\left(\ln \phi_{hs} + \frac{\phi_{hs}(4 - 3\phi_{hs})}{(1 - \phi_{hs})^2} - 1 + \ln (v_o/v_{hs}) + \frac{A}{2}\phi_{hs}\right) \quad \text{(A11)}$$

Let $\Delta g_m = \Delta G_m/v_t$, and then (A11) becomes

$$\frac{\Delta g_m}{kT} = \frac{\phi_{hs}}{v_{hs}}\left(\ln \phi_{hs} + \frac{\phi_{hs}(4 - 3\phi_{hs})}{(1 - \phi_{hs})^2} - 1 + \ln\left(\frac{v_o}{v_{hs}}\right) + \frac{A}{2}\phi_{hs}\right) \quad \text{(13)}$$

Appendix B

If $A = A(R,T,\xi,\Delta\rho)$, we can write

$$dA = \left(\frac{\partial A}{\partial R}\right)_{T,\xi,\Delta\rho}dR + \left(\frac{\partial A}{\partial T}\right)_{R,\xi,\Delta\rho}dT + \left(\frac{\partial A}{\partial \xi}\right)_{R,T,\Delta\rho}d\xi + \left(\frac{\partial A}{\partial \Delta\rho}\right)_{R,T,\xi}d\Delta\rho \quad \text{(B1)}$$

If we consider the systems where only ξ and R are arranged to change their values, and the other variables are fixed, then (B1) reduces to

$$dA = \left(\frac{\partial A}{\partial R}\right)_{\xi}dR + \left(\frac{\partial A}{\partial \xi}\right)_{R}d\xi$$

Mathematically, it is straightforward to show that

$$\left(\frac{\partial R}{\partial \xi}\right)_A = -\frac{(\partial A/\partial \xi)_R}{(\partial A/\partial R)_\xi}$$

Since we knew experimentally that the attraction strength increased as the penetrable length increased during the interpenetration of microemulsion droplets, we can write

$$\left(\frac{\partial A}{\partial \xi}\right)_R > 0$$

Also, the fact that the attraction increased as R increased allows us to write

$$\left(\frac{\partial A}{\partial R}\right)_{\xi} > 0$$

Therefore

$$\left(\frac{\partial R}{\partial \xi}\right)_{A} < 0$$

For $A = A_c$

$$\left(\frac{\partial R^c}{\partial \xi}\right)_{A=A_c} < 0$$

Similarly

$$\left(\frac{\partial A}{\partial \Delta\rho}\right) > 0$$

as deduced from the observation that the attraction strength increased with increasing molecular volume of oil, so

$$\left(\frac{\partial R}{\partial \Delta\rho}\right)_{A} = -\frac{(\partial A/\partial \Delta\rho)_R}{(\partial A/\partial R)_{\Delta\rho}} < 0$$

For $A = A_c$

$$\left(\frac{\partial R^c}{\partial \Delta\rho}\right)_{A=A_c} < 0$$

Registry No. Span-20, 1338-39-2; Span-40, 26266-57-9; Span-60, 1338-41-6; AOT, 577-11-7; water, 7732-18-5; tridecane, 629-50-5; decane, 124-18-5; 1-heptanol, 111-70-6; hexane, 110-54-3; 1-propanol, 71-23-8; 1-pentanol, 71-41-0; 1-nonanol, 143-08-8; hexadecane, 544-76-3; acrylamide, 79-06-1; 1-dodecanol, 112-53-8; benzene, 71-43-2; toluene, 108-88-3; 1-hexanol, 111-27-3; 1-octanol, 111-87-5.

Formation of Multilayers of Dipalmitoylphosphatidylcholine Using the Langmuir–Blodgett Technique

J. B. Peng,† M. Prakash,† R. Macdonald,‡ P. Dutta,*† and J. B. Ketterson†

Department of Physics and Astronomy and Department of Biochemistry, Molecular Biology, and Cell Biology, Northwestern University, Evanston, Illinois 60208

Received March 12, 1987. In Final Form: June 9, 1987

We have deposited Langmuir–Blodgett multilayers of dipalmitoylphosphatidylcholine onto a mica substrate from the surface of an aqueous solution of uranyl acetate. No transfer could be achieved when the subphase was pure water. X-ray diffraction confirms the formation of multilayers; the distance between bilayers is 57 ± 1 Å.

Phospholipids are essential components of biological membranes, and the Langmuir–Blodgett (LB) technique[1] is a convenient way to build up high-quality lamellar structures of such lipids. The head-to-head tail-to-tail structure of LB films mimics the bilayer structure of biological membranes; an assembly of several hundred stacked model membranes, in principle of unlimited area, can be formed from many ampiphiles by using the LB method. Although the method of drying from solution also forms layered structures (and it is on such samples that multilayer studies are generally performed), these are partly amorphous deposits and cannot compare in structural perfection with that found in many LB films. One example of the use of such improved structures is in spectroscopic (e.g., infrared, Raman) studies. Another is in protein crystallography: some membrane proteins (bacteriorhodopsin is a well-known example) are known to crystallize into two-dimensional arrays within membranes. If the protein molecule does not protrude excessively from the plane of the bilayer, one might expect that a monolayer containing an appropriate fraction of the protein can be built up to form a three-dimensional ordered protein structure. The resulting enhanced X-ray diffraction should permit determination of membrane protein molecular structures.

The most abundant polar lipids are phosphatidylcholine (PC), phosphatidylethanolamine (PE), and phosphatidylserine (PS). The transfer of PE[2,3] and phospholipid mixtures[4] to substrates has been observed, but a report[5] of LB film formation using PC and PS is contradicted by Hasmonay, Caillaud, and Dupeyrat,[6] who used the same techniques but found (as we did) that a layer deposited on one stroke would float off on the reverse stroke. Subsequently, Akutsu, Ikematsu, and Yoshimasa[7] have reported that, while PE forms LB films with relative ease, the transfer of PC is much harder and results in patchy, nonuniform films.

It is commonly known that the presence of ions in the subphase greatly improves LB deposition; Marra and Israelachvili[8] have made direct measurements of the forces between phospholipid bilayers in aqueous environments

* Author to whom correspondence should be sent.
† Department of Physics and Astronomy.
‡ Department of Biochemistry, Molecular Biology, and Cell Biology.

(1) Langmuir, I. *J. Am. Chem. Soc.* **1917**, *39*, 541–566. Blodgett, K. B. *J. Am. Chem. Soc.* **1935**, *57*, 1007–1022. For a review, see: Gaines, G. L. *Insoluble Monolayers at Liquid–Gas Interfaces*; Interscience: New York, 1966.
(2) Nakahara, H.; Fukuda, K.; Akutsu, H.; Kyogoku, Y. *J. Colloid Interface Sci.* **1978**, *65*, 517–520.
(3) Hitchcock, P. B.; Mason, R.; Shipley, G. G. *J. Mol. Biol.* **1975**, *94*, 297–299.
(4) Levine, Y. K.; Bailey, A. I.; Wilkins, M. H. F. *Nature (London)* **1968**, *220*, 577–578.
(5) Green, J. P.; Phillips, M. C.; Shiplay, G. G. *Biochim. Biophys. Acta* **1973**, *330*, 243–253.
(6) Hasmonay, H.; Caillaud, M.; Dupeyrat, M. *Biochem. Biophys. Res. Commun.* **1979**, *89*, 338–344.
(7) Akutsu, H.; Ikematsu, M.; Yoshimasa, Y. *Chem. Phys. Lipids* **1981**, *28*, 149–158.
(8) Marra, J.; Israelachvili, J. *Biochemistry* **1985**, *24*, 4608–4618.

0743-7463/87/2403-1096$01.50/0